8. Carbon cycle

8.1. Terrestrial carbon cycle

The terrestrial biosphere absorbs CO_2 from the atmosphere by producing vegetation and releases CO_2 into the atmosphere by decomposition of soil organic carbon. These processes of the terrestrial biosphere can significantly affect the atmospheric CO_2 concentration. For example, the terrestrial biosphere is considered to enhance future global warming by warming-enhanced decomposition of soil organic carbon (climate–carbon cycle positive feedback, e.g., Friedlingstein et al., 2006). Therefore, the terrestrial carbon cycle process is an essential component of the earth system model for the accurate estimation of climate change. The terrestrial carbon cycle model included in MRI-ESM1 is based on models of the biochemical processes of photosynthesis on the organism-leaf level (Woodward et al., 1995; Sellers et al., 1996) and on a dynamic global vegetation model on the ecosystem-biogeochemical level (Sitch et al., 2003). The model is fundamentally improved from the previous MRI carbon cycle model (Obata, 2007), in which biological processes such as net primary production (NPP) are simply and empirically represented by meteorological factors such as temperature and precipitation and by a simple CO_2 fertilization effect. The simple, empirical processes in the previous model led to overestimation of NPP at higher temperatures, and would thus lead to the underestimation of projected warming. This NPP overestimation should be improved by considering more detailed biochemical and ecosystem processes. The processes of the improved model are briefly described below.

On the leaf level, the model calculates biochemical photosynthesis processes and the dependence of CO_2 exchange on stomatal conductance, which in turn depends on temperature and soil moisture (Woodward et al., 1995). The following information is mainly from Woodward et al. (1995), who describe the methods and parameters of the model in detail. The model is able to simulate the net photosynthetic effects of changes in the photorespiratory rate, for example in response to changes in CO_2 concentration or irradiance. The photosynthetic rate of a leaf is determined by the minimum rate of at least two biochemical processes: [1] the rate of carboxylation W_c due to the amount, kinetic properties, and activation state of ribulose bisphosphate carboxylase-oxygenase (Rubisco), and [2] the rate of carboxylation W_j controlled by the rate of ribulose bisphosphate (RuBP) regeneration in the Calvin cycle, a process that is limited by the rate of electron transport (Farquhar et al., 1980).

The net rate of CO_2 assimilation implied by these biochemical processes is

$$A_b = V_c \left(1 - 0.5 p_o / \tau \, pCO_2 \right) - R_d, \quad (8.1)$$

where the rate of carboxylation $V_c = min(W_c, W_j)$; p_o and pCO_2 are the internal partial pressures of O_2 and CO_2 respectively; τ is the specificity factor of Rubisco for CO_2 relative to O_2; and R_d is the rate of respiration in light due to processes other than photorespiration. Typical values of p_o and R_d are 21 000 Pa and 0.82 μmol m^{-2} s^{-1}. The specificity factor τ depends on temperature: τ (T_k) = exp(−3.949 + 28.99/0.00831T_k), where T_k is absolute temperature.

[1] If Rubisco controls photosynthesis, then the carboxylation rate is a hyperbolic function of pCO_2:

$$W_c = V_c^{max} pCO_2 / [pCO_2 + K_c(1+p_o/K_o)], \quad (8.2)$$

where V_c^{max} is the maximum rate of carboxylation by Rubisco. The parameters K_c and K_o are Michaelis coefficients for carboxylation and the competing process of oxygenation by Rubisco (Farquhar et al., 1980).

[2] If the RuBP regeneration rate controls photosynthesis, then the carboxylation rate depends on the rate of electron transport J:

$$W_j = J \, pCO_2 / 4(pCO_2 + p_o/\tau). \quad (8.3)$$

Irradiance drives the electron transport J (e.g., Farquhar et al., 1980).

Stomatal conductance controls the diffusion of CO_2 from the atmosphere into the intercellular air spaces and thus the supply of CO_2, which affects the rates of carboxylation W_c and W_j. Internal CO_2 adjusts to balance supply by diffusion and demand by biochemical photosynthetic processes.

The CO_2 assimilation rate implied by the diffusion gradient in the CO_2 concentration from the atmosphere to the intercellular air spaces is

$$A_d = (pCO_{2\,air} - pCO_2) \, g_s/160, \quad (8.4)$$

where A_d is the CO_2 assimilation rate (μmol m^{-2} s^{-1}), g_s is stomatal conductance to water vapor (mmol m^{-2} s^{-1}), and pCO_{2air} is atmospheric CO_2 partial pressure (Pa). The stomatal conductance is empirically derived from environmental conditions, modified to account for the effects of soil moisture: g_s = ($g_0(T)$ + $g_1(T)AR_h/pCO_{2air}$) $k_g(w_s)$, where R_h is the relative humidity of the air surrounding the leaf and A is the CO_2 assimilation rate. The parameter g_0 is the stomatal conductance when A_d is zero at the light compensation point, and g_1 is an empirical sensitivity coefficient. The function $k_g(w_s)$ describes the response of stomatal conductance to soil water content w_s.

The internal CO_2 partial pressure, pCO_2, is determined by iteratively solving the nonlinear equation that arises by setting the assimilation rate implied by the diffusion gradient (Eq. (8.4)) equal to the assimilation rate indicated by biochemical processes (Eq. (8.1)) with carboxylation rate V_c equal to the minimum of W_c and W_j.

The model described above is for C_3 photosynthesis plants. In the case of C_4 photosynthesis plants, the model can be extended by incorporating a corresponding representation of C_4 photosynthesis (Sellers et al., 1996; Haxeltine and Prentice, 1996), in which CO_2 fertilization is saturated. The leaf-level photosynthesis model is calculated with a time interval of 30 minutes to 1 hour in conjunction with the land-surface model (Section 3.6) of the AGCM. The calculated stomatal conductance is used for water and latent heat fluxes to the atmosphere in the land-surface model. The calculated net photosynthesis is averaged over a day or a month and then used to drive the following vegetation model.

On the ecosystem level, the terrestrial biosphere is subdivided into leaves, stems, roots, litter, and humus. The driving input for the ecosystem is NPP (gross primary production minus plant maintenance respiration), which is partitioned among leaves, stems, and roots. The carbon content of each component is predicted by the carbon outflow equivalent to its fractional content, depending on the component's turnover time, and by carbon inflow from the donor component. The exchange of CO_2 between the atmosphere and the ecosystem is evaluated by the difference between NPP and soil respiration. These calculations are carried out in each terrestrial grid of the AGCM. These basic model structures are the same as in the previous model (Obata, 2007). In the improved model, the vegetation consists of 10 plant functional types (PFTs): 8 woody (2 tropical, 3 temperate, 3 boreal) and 2 herbaceous (tropical, temperate) types. Responses of the PFTs, litter, and humus are calculated with formulations similar to those in the Lund-Potsdam-Jena Dynamic Global Vegetation Model (Sitch et al., 2003), who describe the methods and parameters in detail.

Each PFT population is characterized by a set of variables describing the state of the average individual, and by the population density. For woody PFTs, the average individual is defined by its crown area (m^2) and the sizes of three tissue pools (gC): leaf mass, sapwood mass, and fine root mass. Herbaceous PFTs are treated more simply: population density is arbitrarily set to 1, so that leaf mass and fine root mass represent grid cell area averages ($gC\ m^{-2}$), and sapwood is undefined. Above- and below-ground litter carbon pools with a turnover time of about 3 years and 2 soil carbon pools with intermediate (~30 years) and slow (~1000 years) turnover times are defined for the entire grid cell.

In the calculation, maintenance and growth respiration are subtracted from net photosynthesis, obtained from the leaf-level biochemical model described above, and tissue turnover reduces individual plant biomass, with dead leaf and root tissue entering the litter pools. The remaining photosynthate is allocated to the vegetation parts, satisfying allometric relationships. Litter and soil organic matter decomposition are driven by seasonal temperatures and soil moisture status. These calculations are carried out for a time interval of 1 day to 1 month. Population densities are updated annually based on establishment and mortality. If 20-year mean values of bioclimatic variables fall outside the PFT's survival limits, the entire population is killed.

In a preliminary trial, the terrestrial carbon cycle model described above was included in an MRI climate-carbon cycle model (Obata, 2007) based on MRI-CGCM2 (Yukimoto and Kitamura, 2003) instead of the previous simple terrestrial carbon cycle model. The preindustrial steady state is well reproduced, with high values of NPP and leaf area index in the tropics because of the warm, wet conditions (Fig. 14), and a global NPP of 56 GtC yr^{-1}, consistent with previous estimates (e.g., Prentice et al., 2001).

8.2. Oceanic Carbon Cycles

Biogeochemical models [see Tsujino et al., 2010, for details] are composed of inorganic carbon-cycle and ecosystem component models. In the inorganic carbon-cycle component, pCO_2 at the sea surface is determined from dissolved inorganic carbon (DIC) and Alkalinity (Alk) values at the sea surface, which needs the ecosystem component. The difference in pCO_2 between the atmosphere and ocean determines uptake or release of CO_2 from the ocean to the atmosphere, and is essential for simulating the CO_2 concentration in the atmosphere. Inorganic carbonate chemistry and partial pressure physics are well understood and can be reproduced with fair accuracy. The ecosystem component treats various biological activities, and gives sources and sink of the nutrients, DIC, Alk, and dissolved oxygen through these activities, but our knowledge of them is far from complete.

The ocean ecosystem model is based on Oschiles (2001). The prognostic variables for the ecosystem model are phytoplankton (P), zooplankton (Z), detritus(D), dissolved Inorganic Nitrate (NO_3), dissolved inorganic phosphate (PO_4), and dissolved oxygen (O_2). The Tracer concentrations follow advective diffusive equations with source-minus-sink (SMS) terms of exchange between different

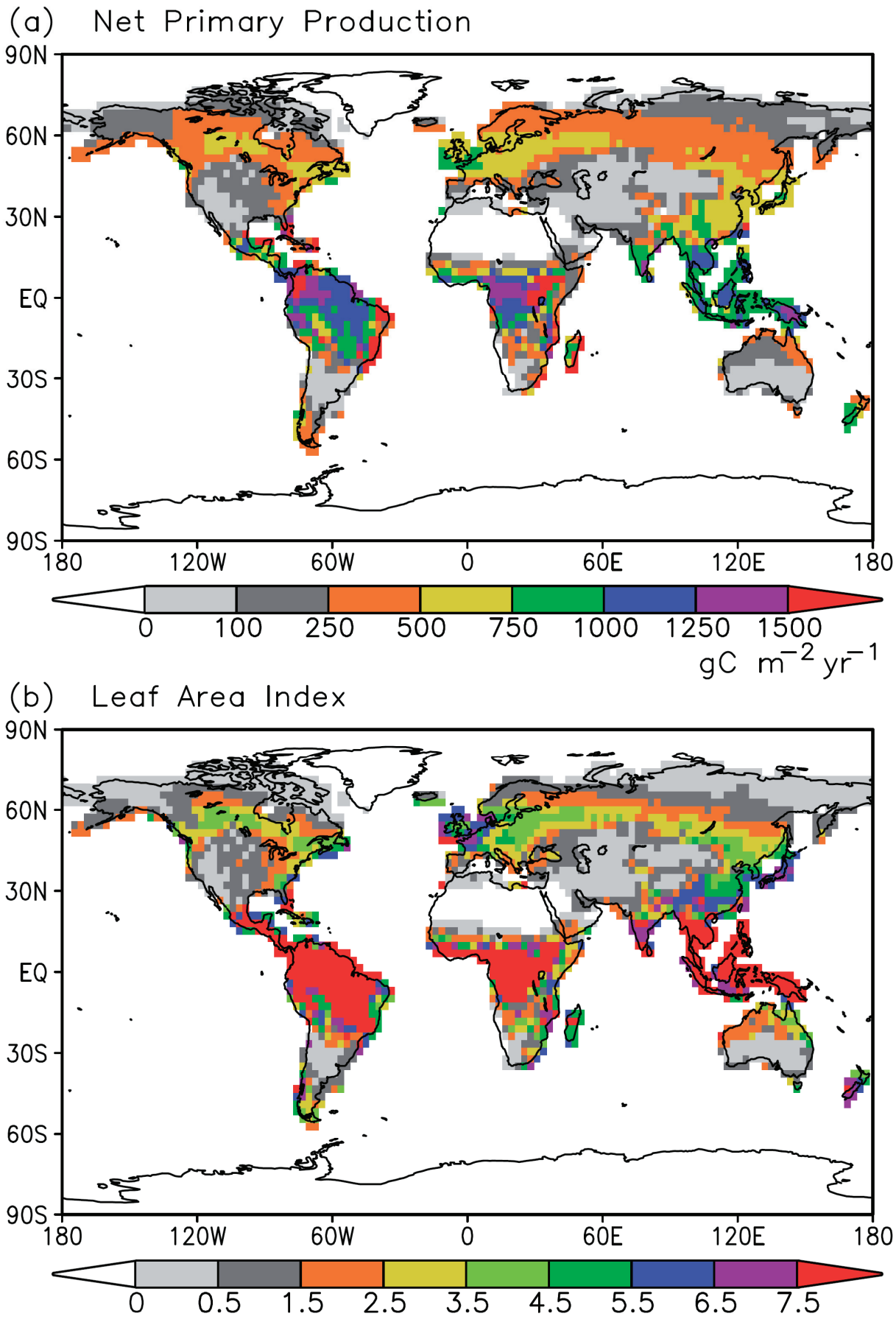

Figure 14 (a) Net primary production and (b) leaf area index in the preindustrial state of the land carbon cycle model.

tracers. The units of the SMS terms are (mol $m^{-3}s^{-1}$).

$$
\begin{aligned}
SMS(P) &= J(I, NO_3, PO_4)P - \varphi_P P - \varphi_{PP} P^2 - G(P)Z \\
SMS(Z) &= f_a G(P)Z - \varphi_Z Z - \varphi_{ZZ} Z^2 \\
SMS(D) &= (1 - f_a)G(P)Z + \varphi_{PP} P^2 + \varphi_{ZZ} Z^2 - \varphi_D D - w_D \frac{\partial D}{\partial z} \\
SMS(NO_3) &= \varphi_P P + \varphi_Z Z + \varphi_D D - J(I, NO_3, PO_4)P \\
SMS(PO_4) &= SMS(NO_3) \cdot R_{pn} \\
SMS(O_2) &= -SMS(PO_4) \cdot R_{on} \cdot R_{np}
\end{aligned}
\qquad (8.5\text{-}8.10)
$$

Here, the grazing function $G(P)$ is $g\varepsilon P^2 / (g + \varepsilon P^2)$. Other variables and their values are listed in Table 4.

The growth rate of phytoplankton $J(I,NO_3,PO_4)$ is limited by either light or and nutrient levels. For the nutrient limitation, we adopt optimal uptake kinetics, which assumes a physiological trade-off between the efficiency of nutrient encounters at the cell surface and the maximum assimilation rate (Smith et al., 2009).

$$J_I = \frac{J_{\max} \alpha I}{[J_{\max}^2 + (\alpha I)^2]^{1/2}} \qquad (8.12)$$

$$I = I_{z=0} PAR \exp(-k_w \tilde{z} - k_e \int_0^{\tilde{z}} P dz) \qquad (8.13)$$

$$J_{\max} = a \cdot b^{cT} \qquad (8.14)$$

$$J_N = \frac{V_o N}{N + 2\sqrt{\alpha_{OU} N} + \alpha_{OU}} \qquad (N = NO_3 \ \ or \ \ PO_4) \qquad (8.15)$$

$$V_o = 0.5(1 + \sqrt{\frac{\alpha_{OU}}{K_N}}) \qquad (8.16)$$

Here, $\tilde{z} = z/\cos\theta = z / (sin2\theta / 1.33^2)^{1/2}$ is the effective vertical coordinate for a refraction index of 1.33 according to Snell's law relating the zenith angle of incidence in air (θ) to the angle of incidence in water.

Formulations for the production of DIC and Alk are based on Schmittner et al. (2008, 2009). Production changes in inorganic nutrients and calcium carbonate ($CaCO_3$), in molar numbers, are

Table 4 Notations and their values in the terrestrial carbon cycle model

notation	description	units	value
α	Initial slope of P-I curve	$(W\ m^{-2})^{-1}\ day^{-1}$	0.1d0
a	Maximum growth rate parameter	day^{-1}	0.2d0
b	Maximum growth rate = ab^{cT}		1.066d0
c			1.d0
PAR	Photosynthetically active radiation		0.43d0
k_e	Light attenuation due to phytoplankton	$m^{-1}\ (mol\ m^{-3})^{-1}$	0.03d3
k_w	Light attenuation in the water	m^{-1}	0.04d0
k_{NO3}	Half-saturation constant for NO_3 uptake	$mol\ m^{-3}$	0.7d-3
k_{PO4}	Half-saturation constant for PO_4 uptake	$mol\ m^{-3}$	0.d0
α_{OU}	Fitting constant for Optical Uptake kinetics		0.19d0
g	Maximum grazing rate	day^{-1}	1.575d0
ε	Prey capture rate	$(mol\ m^{-3})^{-2}\ day^{-1}$	1.6d6
φ_P	Specific mortality/recycling rate	s^{-1}	0.014d0
φ_{PP}	Quadratic mortality rate	$(mol\ m^{-3})^{-1}\ day^{-1}$	0.05d3
f_a	Assimilation efficiency		0.925d0
φ_{ZZ}	Quadratic mortality of zooplankton	$(mol\ m^{-3})^{-1}\ day^{-1}$	0.34d3
φ_Z	Excretion	day^{-1}	0.01d0
φ_D	Remineralization rate	day^{-1}	0.048d0
w_D	Sinking velocity	$m\ day^{-1}$	2.d0
R_{cn}	Molar elemental ratio (C/N)		7.d0
R_{on}	Molar elemental ratio (O_2/N)		10.d0
R_{np}	Molar elemental ratio (N/P)		16.d0
$R_{caco3/poc}$	$CaCO_3$ over nonphotosynthetic POC production ratio		0.05d0
D_{caco3}	$CaCO_3$ remineralization e-folding depth	m	3500.d0

$$SMS(DIC) = Sb(PO_4) \cdot R_{CP} - Sb(CaCO_3)$$
$$SMS(Alk) = -Sb(NO_3) - 2 \cdot Sb(CaCO_3) \qquad (8.17\text{-}8.19)$$
$$SMS(CaCO_3) = \Pr(CaCO_3) - Di(CaCO_3)$$

$$\Pr(CaCO_3) = ((1 - f_a)G(P)Z + \varphi_{PP}P^2 + \varphi_{ZZ}Z^2) \cdot R_{CaCO_3/POC} \cdot R_{CN} \qquad (8.20)$$

$$Di(CaCO_3) = \int \Pr(CaCO_3)dz \cdot \frac{d}{dz}(\exp(-z / D_{CaCO_3})) \qquad (8.21)$$

Formulations of air-sea gas exchange and carbon chemistry follow protocols of the Ocean Carbon-Cycle Model Intercomparison Project (Orr et al., 1999).